

Faithful Solid State Optical Memory with Dynamically Decoupled Spin Wave Storage

Marko Lovrić,^{1,2,*} Dieter Suter,¹ Alban Ferrier,² and Philippe Goldner^{2,†}

¹*Technische Universität Dortmund, Fachbereich Physik, D-44221 Dortmund, Germany*

²*Chimie ParisTech, Laboratoire de Chimie de la Matière Condensée de Paris, CNRS-UMR 7574, UPMC Univ Paris 06, 11 rue Pierre et Marie Curie 75005 Paris, France*

(Dated: January 25, 2018)

We report an optical memory in a rare earth doped crystal with long storage times, up to 20 ms, together with an optical bandwidth of 1.5 MHz. This is obtained by transferring optical coherences to nuclear spin coherences, which were then protected against environmental noise by dynamical decoupling. With this approach, we achieved a 33 fold increase in spin wave storage time over the intrinsic spin coherence lifetime. Comparison between different decoupling sequences indicates that sequences insensitive to initial spin coherence increase retrieval efficiency. Finally, an interference experiment shows that relative phases of input pulses are preserved through the whole storage process with a visibility ≈ 1 , demonstrating the usefulness of dynamical decoupling for extending the storage time of quantum memories.

PACS numbers: 03.67.Pp, 42.50.Md, 03.67.Hk

Quantum memories for light (QML) are devices capable of faithfully storing photonic quantum states into atomic states [1]. Their applications include long distance quantum cryptography and more generally quantum networks [2]. Besides atomic vapors, rare earth ions have recently been considered as promising candidates for solid state QMLs. This is because of the coherence lifetimes of their optical and nuclear spin transitions, which can reach the ms range [3, 4]. Moreover, these systems are well suited for memories with large time-bandwidth products since their optical inhomogeneous linewidth can exceed by several orders of magnitude the homogeneous one [3]. To take advantage of this property, the optical input signal is absorbed in an inhomogeneously broadened transition. Excited atomic coherences then dephase and, after a time t , are rephased by an optical control pulse, resulting in an output signal at time $2t$ similar to a photon echo [5]. Protocols like CRIB (Controlled Reversible Inhomogeneous Broadening) [6], GEM (Gradient Echo Memory) [7], AFC (Atomic Frequency Comb) [8, 9] or ROSE (Revival of Silenced Echo) [10] have been developed from this basic scheme to allow for high efficiency, high bandwidth and single photon level input signals. To reach long storage times, the optical coherence can be transferred to a ground state nuclear spin coherence. This is also required in the AFC protocol to obtain an on-demand memory [11]. Using these protocols in different rare earth crystals, recent demonstrations include 1 GHz bandwidth storage [12], 70 % storage efficiency [13], entanglement storage [14, 15] and entanglement of two crystals [16]. However, the few experiments on optical to spin storage reported storage times of only $\approx 20 - 50 \mu\text{s}$ [11, 17, 18]. In these studies, however, the spin coherence was not refocused and the storage time was therefore limited by the spin inhomogeneous broadening. On the other hand, it has been shown that very efficient control of rare

earth spin decoherence can be achieved by combining external magnetic fields [19, 20] and dynamical decoupling with radio-frequency (RF) pulses [21, 22]. In demonstrations using electromagnetically induced transparency (EIT), this lead to memories with storage times up to several seconds [23, 24]. However, EIT is seriously limited in bandwidth because of the low oscillator strength of rare earth transitions, and the largest bandwidths reported in these memories do not exceed a few tens of kHz. Here, we demonstrate a photon echo based memory in a rare earth doped crystal with a bandwidth of 1.5 MHz and storage times between 7 and 20 ms, increasing previous values up to three orders of magnitude. This is achieved by controlling spin coherence by RF dynamical decoupling (DD) sequences. Comparison between these sequences reveals that sequences insensitive to initial spin coherence increase retrieval efficiency. We finally investigated storage fidelity, a crucial point in quantum memories, and show that relative optical phases are preserved through the whole storage process. This result provides the first demonstration of high fidelity storage in an ensemble-based optical memory using dynamical decoupling. This shows the high potential of this technique for ensemble-based memories in general.

Experiments were performed on a 0.2 at.% $\text{Pr}^{3+}:\text{La}_2(\text{WO}_4)_3$ single crystal. This material was developed for quantum memories to reach low optical inhomogeneous broadening at high Pr^{3+} concentration in order to increase optical depth [25, 26]. The crystal was cooled down to a temperature of ≈ 5 K in a cold finger liquid helium cryostat. Optical excitation was provided by a Coherent 899-21 dye laser stabilized to a linewidth < 20 kHz. Light propagated parallel to the crystal b axis and was focused to a spot of $40 \mu\text{m}$ inside the sample which was 4 mm thick. Optical pulse amplitude and frequency were controlled by acoustic-optic

modulators (AOM) in double pass configuration, driven by an arbitrary waveform generator. The signal was detected by an avalanche photodiode. To apply radio frequency (RF) pulses, a 6 mm, 10 turn coil surrounded the crystal. To reduce reflections and increase the field strength, the coil was part of a tuned circuit, which was driven with maximum RF power of 9 W and controlled by a 300 MS/s direct digital synthesizer.

Optical excitations were resonant with transitions between the lowest electronic level of the $\text{Pr}^{3+} \ ^3\text{H}_4$ ground and the $^1\text{D}_2$ excited state multiplet (Fig. 1, upper part). The optical transition has an inhomogeneous linewidth of 10 GHz and a homogeneous one of 27 kHz ($T_2 = 11.5 \ \mu\text{s}$). $^{141}\text{Pr}^{3+}$ has a $I = 5/2$ nuclear spin and 100% abundance. Each electronic level has a hyperfine structure of three doubly degenerate levels (Fig. 1, upper part) at zero external magnetic field. The strongest optical transition occurs between levels (i) and (e) [27] and was chosen to absorb the input signal. Spin storage was performed on the (i)-(t) transition at 14.87 MHz.

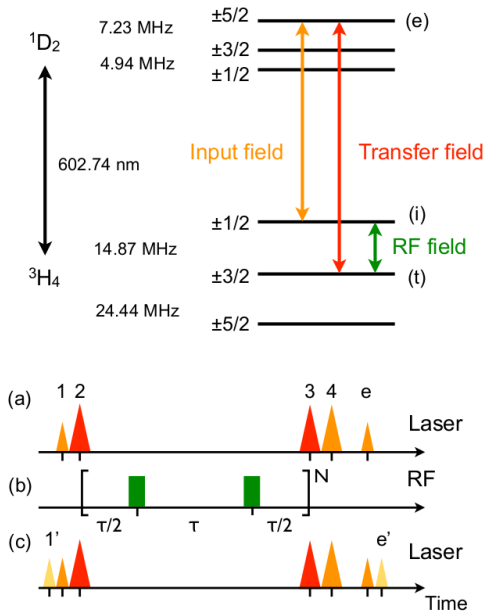


FIG. 1. (Color online) Upper part: hyperfine structure of $\text{Pr}^{3+} \ ^3\text{H}_4$ and $^1\text{D}_2$ levels in $\text{Pr}^{3+}:\text{La}_2(\text{WO}_4)_3$ and transitions used in this work. Lower part: laser sequences for one (a) or two (c) pulse storage. Pulses 1 and 4 were gaussian with full width at half maximum (FWHM) lengths of 200 and 425 ns respectively. Pulses 2 and 3 were secant hyperbolic with FWHM length of $2.25 \ \mu\text{s}$ and a 2 MHz chirp. The delay t_{12} , between pulse 1 and 2, and t_{34} were set to $2 \ \mu\text{s}$. Comparing echo intensity with and without transfer pulses, we deduced a transfer efficiency for fields of 87 % per pulse. (b) RF pulse sequence for hyperfine transition dynamical decoupling; the basic block showed in bracket is repeated N times (see text).

As the optical inhomogeneous linewidth is much larger

than the hyperfine level separation, optical pumping was first used to isolate the transitions of interest. The first step of the optical pumping sequence [27] consisted in burning a spectral pit of 25 MHz, to empty levels (i) and (t) for one class of ions. Population was then brought back into the (i) level of these ions by a pulse adjusted to create a 1.5 MHz wide absorption peak. Finally, additional pulses were applied to remove unwanted spectral features in the pit. Fig. 2 shows the final transmission spectrum at the end of the preparation sequence. It consists of a well isolated peak at 12.2 MHz corresponding to the (i)-(e) transition and a low background absorption on the (t)-(e) transition at 27.0 MHz. Level (t) is therefore empty, which is required for efficient transfer of the optical (i)-(e) coherence to the hyperfine (i)-(t) transition.

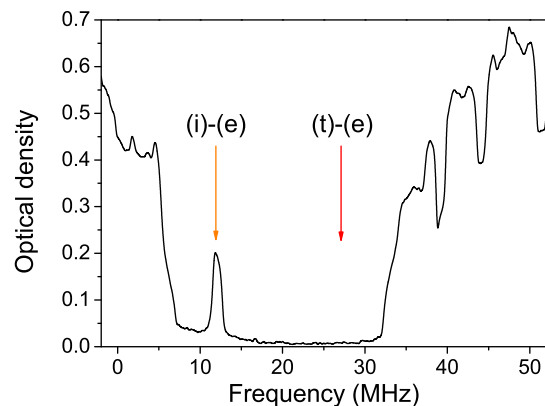


FIG. 2. Absorption spectrum after optical pumping.

Fig. 1 (a) and (b) show the general memory sequence that we used. The input signal (pulse 1) was first absorbed by the inhomogeneously broadened (i)-(e) transition. The resulting coherence was then transferred to the hyperfine (i)-(t) coherence by a π pulse resonant with the (t)-(e) transition (pulse 2). The inhomogeneous dephasing of the resulting initial spin coherence was refocused by an even number of RF π pulses applied to the (i)-(t) transition (see Fig. 1 (b)). If the pulses are applied at a rate larger than the correlation time of the dephasing bath, the spin transition coherence lifetime may increase through dynamical decoupling [28]. This is because the bath appears static, like an additional inhomogeneous broadening, between successive π pulses. The RF pulses refocus this broadening and effectively increase the transition coherence lifetime. Ideally, after the last RF pulse and a delay of $\tau/2$, where τ is the RF pulse separation, the hyperfine coherence state is the same as the initial one. Applying a second transfer at this time (pulse 3) brings the hyperfine coherence back to the optical domain. A final π pulse along the (i)-(e) transition (pulse

4), refocuses the optical dephasing of the coherence. Finally, the output signal (pulse e) appears as a photon echo at a time $t_{4e} = t_{12} + t_{34}$ after pulse 4, where t_{ij} is the delay between pulses i and j . The memory storage time is $T = t_{1e}$.

RF pulses of rectangular shape were applied between the transfer pulses as shown in Fig. 1 (a) and (b). Using an appropriate RF power the pulse area was set to π , while their duration was set to $5 \mu\text{s}$ so that their spectral width ($\approx 200 \text{ kHz}$) was larger than the inhomogeneous linewidth of the (i)-(t) transition (45 kHz). The pulse amplitude was determined by nutation and spin echo experiments. The relative phase of successive RF pulses could be adjusted, X and Y representing respectively 0 and 90° phases in the following. The optical phase of the laser was independent of the RF phase, thus for each repetition of the experiment the initial phase of the spins was arbitrary compared to the RF pulse phases. Moreover, since the first transfer pulse was applied after evolution in the optical domain, there was a distribution of initial spin phases. As a result, no spin echo was observed between RF pulses or at the end of the RF sequence. Only the final optical echo could be used to probe the spin coherence decay. The RF sequences consisted of a basic block of length 2τ , which was repeated N times (see Fig. 1 (b)).

We compared two dynamical decoupling sequences. Their building blocks, where e.g. $\pi(\phi)$ represents a RF π pulse with ϕ phase, are given by: (i) $[\tau/2 - \pi(X) - \tau - \pi(X) - \tau/2]$, Carr-Purcell-Meiboom-Gill (CPMG) sequence [29]; (ii) $[\text{KDD}(X) - \text{KDD}(Y) - \text{KDD}(X) - \text{KDD}(Y)]$, where $\text{KDD}(\phi) = [\tau/2 - \pi(\phi + \pi/6) - \tau - \pi(\phi) - \tau - \pi(\phi + \pi/2) - \tau - \pi(\phi) - \pi(\phi + \pi/6) - \tau/2]$, Knill DD (KDD) sequence [30]. The CPMG sequence has one of the highest decoupling efficiencies, but only when the spins are initially aligned with the rotation axis of the pulses [31]. The KDD sequence is designed to be insensitive to initial phases [30].

Figure 3 shows the output signal intensity I as a function of the storage time T for the CPMG and KDD sequences. I is normalized to the output pulse obtained with zero delay between transfer pulses and no RF pulses, and is plotted as a retrieval efficiency. The pulse separation τ was $30 \mu\text{s}$ for KDD and CPMG sequences and was optimized for the longest storage time with KDD. As shown in Fig. 3, output signal decays were approximately exponential with corresponding effective coherence lifetimes $T_{2,\text{eff}}$ of 8.4 ms and 1.9 ms for CPMG and KDD sequences respectively. $T_{2,\text{eff}}$ is defined by the decay of the optical echo intensity I as a function of storage time T , $I = I_0 \exp(-2T/T_{2,\text{eff}})$. Compared to using only 2 RF pulses ($T_{2,\text{eff}} = 230 \mu\text{s}$), i.e. refocusing only the static inhomogeneous spin broadening, the two DD sequences significantly increase the storage time $T_{2,\text{eff}}$ (see Fig. 3). A signal to noise ratio of 2 after 200 accu-

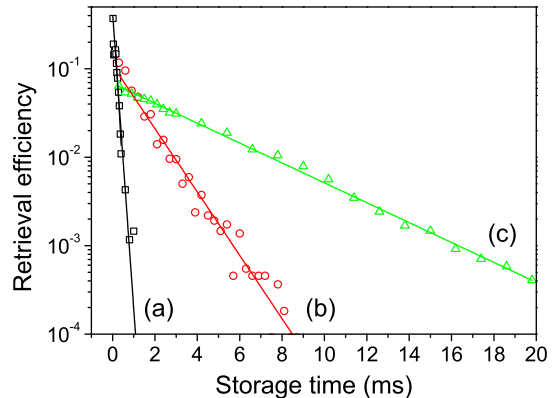


FIG. 3. Retrieval efficiency as a function of storage time using two RF pulses (a), KDD (b) and CPMG (c) dynamical decoupling sequences. The retrieval efficiency is normalized to the echo intensity extrapolated at zero delay, using transfer pulses but no RF pulses.

mulations is reached at a storage time $T = 20 \text{ ms}$ for CPMG and at $T = 7 \text{ ms}$ for KDD. CPMG provides the longest relaxation time, since it 'locks' the spins along the effective field generated by the pulses. However, at $300 \mu\text{s}$ storage time, KDD's retrieval efficiency is nearly twice the one obtained with CPMG (12 % and 6.4 % respectively). This can be explained by the initial distribution of spin phases at the input of the DD sequences (see above): CPMG preserves only the component of the spin which is initially oriented along the rotation axis of the pulses, while KDD protects all spin components and therefore the full quantum state, as required for a quantum memory [30].

We finally checked the fidelity of the memory by storing two optical pulses [32]. As the laser coherence lifetime is only about $50 \mu\text{s}$, the phase of the output pulses from identically repeated experiments are random. Only relative phases between successive (within $\approx 50 \mu\text{s}$) input and output pulses are therefore relevant. The used sequence is shown in Fig. 1 (c) and (b). Compared to sequence (a), an additional gaussian pulse (pulse 1') of 200 ns FWHM duration is stored in the memory with a delay $t_{1'1} = 1 \mu\text{s}$. The RF DD sequence followed the KDD scheme with $\tau = 30 \mu\text{s}$ and a storage time of 3 ms . As the spectral width of the input pulses was about 5 MHz , but the prepared absorption line ((i)-(e), see Fig. 2) was only 1.5 MHz wide, the output pulses e and e' were broadened to 400 ns and therefore overlapped in time and interfered. Fig. 4 (a), (b), (c) shows the overlapping output pulses when the relative phase of the input pulses is 0 , -270 and -180° respectively. The output intensities were well modeled by two overlapping gaussian pulses (see Fig. 4 (a), (b), (c)), confirming the origin of the out-

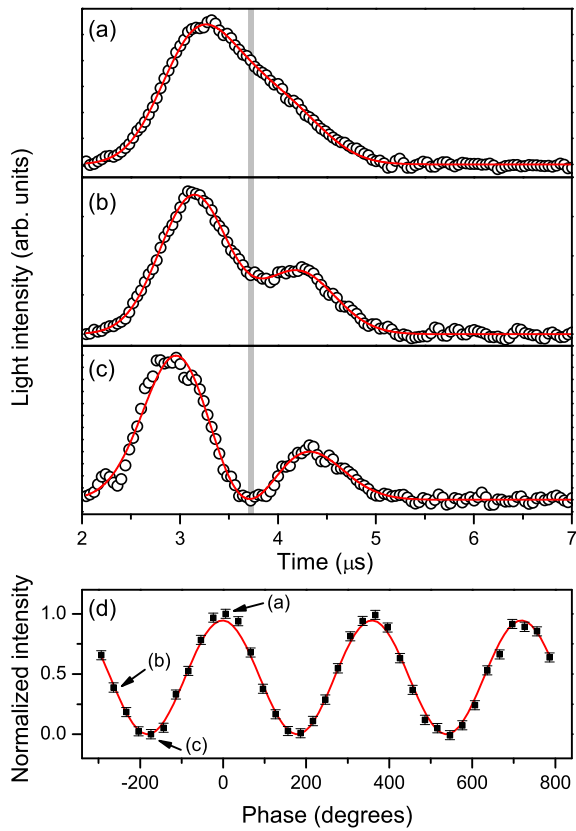


FIG. 4. Interfering output pulses after storage of two input pulses, with 0° (a), -270° (b) and -180° (c) relative phases, for 3 ms. Open circles: experimental data, solid line: fit using two gaussian pulses. (d) Normalized output light intensity averaged at $3.7 \mu\text{s}$ over 50 ns (gray area in (a)-(c)) as a function of the relative input pulse phase. Squares: experimental data, solid line: fit with a visibility expression (see text).

put signal variations. Light intensity was then averaged over 50 ns around the center of the interfering region (see Fig. 4 (a), (b), (c)) and normalized. This intensity $I_n(\phi)$ is plotted against the input pulses relative phase ϕ in Fig. 4 (d) and was well fitted by the visibility expression $I_n(\phi) = (I_{\text{max}}/2)(1 + V \sin(\phi))$ with $V = 0.99$. Relative phases are therefore preserved through the whole storage process, which is a key requirement for a quantum memory. Similar results were obtained with the CPMG sequence with storage times up to 10 ms.

In conclusion, we have demonstrated the feasibility of coherence transfer to spin states and control by dynamical decoupling to drastically extend the storage time in a high bandwidth photon echo based optical memory. Depending on the decoupling sequence, storage times between 7 and 20 ms have been achieved together with an

optical bandwidth of 1.5 MHz. We found that decoupling sequences insensitive to initial spin states, such as KDD, increase the retrieval efficiency. Finally, we demonstrated that the relative phase of input pulses was preserved through the whole storage process, as was shown by storing two input pulses which are allowed to interfere at the output of the memory. This key property allows considering application of these techniques to extend storage times of ensemble-based quantum memories.

The authors thank Mikael Afzelius for useful discussions. This work was supported by the European Union FP7 projects QuRep (247743) and CIPRIS (Marie Curie Action - 287252).

* Present address: Sirah Lasertechnik GmbH, Heinrich-Hertz-Straße 11, D-41516 Grevenbroich, Germany

† philippe-goldner@chimie-paristech.fr

- [1] A. I. Lvovsky, B. C. Sanders, and W. Tittel, *Nature Photonics* **3**, 706 (2009).
- [2] H. J. Kimble, *Nature* **453**, 1023 (2008).
- [3] R. M. Macfarlane, *J. Lumin.* **100**, 1 (2002).
- [4] A. L. Alexander, J. J. Longdell, and M. J. Sellars, *J. Opt. Soc. Am. B* **24**, 2479 (2007).
- [5] W. Tittel, T. Chanelière, R. L. Cone, S. Kröll, S. A. Moiseev, and M. Sellars, *Laser & Photon. Rev.* **4**, 244 (2009).
- [6] M. Nilsson and S. Kröll, *Opt. Comm.* **247**, 393 (2005).
- [7] G. Hétet, J. Longdell, A. Alexander, P. Lam, and M. Sellars, *Phys. Rev. Lett.* **100**, 023601 (2008).
- [8] H. de Riedmatten, M. Afzelius, M. U. Staudt, C. Simon, and N. Gisin, *Nature* **456**, 773 (2008).
- [9] M. Afzelius, C. Simon, H. de Riedmatten, and N. Gisin, *Phys. Rev. A* **79**, 052329 (2009).
- [10] V. Damon, M. Bonarota, A. Louchet-Chauvet, T. Chanelière, and J.-L. Le Gouët, *New J. Phys.* **13**, 093031 (2011).
- [11] M. Afzelius, I. Usmani, A. Amari, B. Lauritzen, A. Walther, C. Simon, N. Sangouard, J. Minář, H. de Riedmatten, and N. Gisin, *Phys. Rev. Lett.* **104**, 40503 (2010).
- [12] M. Bonarota, J.-L. Le Gouët, and T. Chanelière, *New J. Phys.* **13**, 013013 (2011).
- [13] M. P. Hedges, J. J. Longdell, Y. Li, and M. J. Sellars, *Nature* **465**, 1052 (2010).
- [14] C. Clausen, I. Usmani, F. Bussièrès, N. Sangouard, M. Afzelius, H. de Riedmatten, and N. Gisin, *Nature* **469**, 508 (2011).
- [15] E. Saglamyurek, N. Sinclair, J. Jin, J. A. Slater, D. Oblak, F. Bussièrès, M. George, R. Ricken, W. Sohler, and W. Tittel, *Nature* **469**, 512 (2011).
- [16] I. Usmani, C. Clausen, F. Bussièrès, N. Sangouard, M. Afzelius, and N. Gisin, *Nat Photon* **6**, 234 (2012).
- [17] M. Mazzerà, P. M. Ledingham, M. Cristiani, and H. de Riedmatten, *arXiv quant-ph* (2013).
- [18] N. Timoney, I. Usmani, P. Jobez, M. Afzelius, and N. Gisin, *arXiv quant-ph* (2013).
- [19] E. Fraval, M. Sellars, and J. Longdell, *Phys. Rev. Lett.* **92**, 077601 (2004).
- [20] M. Lovrić, P. Glasenapp, D. Suter, B. Tumino, P. Gold-

- ner, M. Sabooni, L. Rippe, and S. Kröll, *Phys. Rev. B* **84**, 104417 (2011).
- [21] E. Fraval, M. Sellars, and J. Longdell, *Phys. Rev. Lett.* **95**, 030506 (2005).
- [22] M. Pascual-Winter, R. C. Tongning, T. Chanelière, and J.-L. Le Gouët, *Phys. Rev. B* **86**, 184301 (2012).
- [23] J. J. Longdell, E. Fraval, M. J. Sellars, and N. B. Manson, *Phys. Rev. Lett.* **95**, 063601 (2005).
- [24] G. Heinze, A. Rudolf, F. Beil, and T. Halfmann, *Phys. Rev. A* **81**, 011401 (2010).
- [25] F. Beaudoux, O. Guillot-Noël, J. Lejay, A. Ferrier, and P. Goldner, *J. Phys. B: At. Mol. Opt. Phys.* **45**, 124014 (2012).
- [26] P. Goldner, O. Guillot-Noël, F. Beaudoux, Y. Le Du, J. Lejay, T. Chanelière, L. Rippe, A. Amari, A. Walther, and S. Kröll, *Phys. Rev. A* **79**, 033809 (2009).
- [27] O. Guillot-Noël, P. Goldner, F. Beaudoux, Y. Le Du, J. Lejay, A. Amari, A. Walther, L. Rippe, and S. Kröll, *Phys. Rev. B* **79**, 155119 (2009).
- [28] L. Viola and S. Lloyd, *Phys. Rev. A* **58**, 2733 (1998).
- [29] S. Meiboom and D. Gill, *Rev. Sci. Instrum.* **29**, 688 (1958).
- [30] A. Souza, G. Álvarez, and D. Suter, *Phys. Rev. Lett.* **106**, 240501 (2011).
- [31] A. M. Souza, G. A. Álvarez, and D. Suter, *Phil. Trans. R. Soc. A* **370**, 4748 (2012).
- [32] M. Lovrić, , Ph.D. thesis, Technical University of Dortmund (2011).